Numerical Simulation of Conjugated Heat Transfer Characteristics of Laminar Air Flows in Parallel-Plate Dimpled Channels

Hossein Shokouhmand , Mohammad A. Esmaeili, Koohyar Vahidkhah

Abstract—This paper presents a numerical study on surface heat transfer characteristics of laminar air flows in parallel-plate dimpled channels. The two-dimensional numerical model is provided by commercial code FLUENT and the results are obtained for channels with symmetrically opposing hemi-cylindrical cavities onto both walls for Reynolds number ranging from 1000 to 2500. The influence of variations in relative depth of dimples (the ratio of cavity depth to the cavity curvature diameter), the number of them and the thermo-physical properties of channel walls on heat transfer enhancement is studied. The results are evident for existence of an optimum value for the relative depth of dimples in which the largest wall heat flux and average Nusselt number can be achieved. In addition, the results of conjugation simulation indicate that the overall influence of the ratio of wall thermal conductivity to the one of the fluid on heat transfer rate is not much significant and can be ignored.

Keywords—cavity, conjugation, heat transfer, laminar air flow, Numerical, parallel-plate channel.

I. INTRODUCTION

FORCED convection laminar flows in parallel-plate channels have been widely studied in recent decades. This problem is encountered in applications such as compact heat exchangers and electronic equipment packages that are involved with space or weight limitations.

In most parallel-plate channels, the flow is laminar due to small channel dimensions and low fluid velocities and as a result heat transfer coefficient is very low. A typical method to enhance this insufficient heat transfer rate is to install transverse ribs normal to the main flow. These ribs interrupt the hydrodynamic boundary layer periodically, add surface area, generate secondary flows and vortexes, and increase flow velocity by decreasing the channel width. It is clear that the enhancement in heat transfer rate is extremely dependent on the arrangement of the ribs and to some extent, on the geometric properties of them. Related studies to this field are accomplished by Kelkar and Patankar [1], Lazaridis [2], and Cheng and Huang [3] who numerically investigated the heat transfer characteristics of periodic fully developed flows in parallel-plate channels with normal fins located on the walls and studied the effect of relative position of the fins on heat

F. H. Shokouhmand, Mech. Eng. Dep., University of Tehran, Tehran, Iran,
S. Mohammad A. Esmaeili, Mech. Eng. Dep., University of Tehran, Tehran, Iran (m.amin.esmaeili@gmail.com),
T. K. Vahidkhah, Med. Eng. Department, Amirkabir University of Technology (Tehran Polytechnic), Tehran, Iran (k.vahidkhah@gmail.com).

transfer enhancement.

Ghaddar et al. [4] numerically studied two dimensional incompressible isothermal cyclic flows in channels with integrated circuits protrusions. Their results showed a critical value for the Reynolds number above which cyclic flow oscillations are observed. Ghaddar et al. [5] used two dimensional incompressible non-isothermal numerical simulations and showed that there is a potential of improving heat transfer by the use of the unsteadiness observed in their previous work.

The inward protruding elements generally increase pressure drop drastically. Thus, in recent years, in design of thermal systems, there has been an increasing tendency to attach arrays of transverse cavities pointing outward onto the walls of parallel-plate channels. The reason is that the increase in undesirable pressure drop in dimpled channels is generally lower compared to the ribbed ones and this is due to more self-structured motion of the fluid in cavities. Heat transfer in these dimpled channels is enhanced due to periodic interruptions of thermal boundary layers and also improvement in lateral mixing by disruption of the shear layer, separation of the bulk flow, formation of recirculating flows, and thus destabilization of the transversal vortices in the dimples.

There are plentiful studies on fluid flows and heat transfer characteristics in the parallel plate channels with periodically dimpled parts. Farhanieh et al. [6] performed numerical and experimental studies on laminar fluid flow and heat transfer characteristics in a duct with a rectangular grooved wall. The results indicated enhancement in the local Nusselt number compared to a smooth parallel plate duct due to re-establishment of thermal boundary layers and formation of recirculating flows inside the grooves. They also showed a relatively high pressure drop increase accompanying this enhancement. Moon et al. [7] investigated the influence of channel height, and showed that when this value is larger than the dimple depth, the dependence of heat transfer enhancement on channel height can be ignored. Chyu et al. [8] studied the cooling passages for turbine blades with circular and teardrop shaped dimples and compared their performance with general turbulence promoters like broken ribs. Their results indicated that both heat transfer enhancement and pressure drop are lower in dimpled channels. Ligrani et al. [9] studied the combined effect of dimples and protrusions on opposite walls and showed that protrusions increase heat transfer and friction

World Academy of Science, Engineering and Technology
International Journal of Mechanical and Mechatronics Engineering
Vol:5, No:1, 2011

coefficients due to increased mixing and vortex stretching.

Herman and Kang [10] investigated the heat transfer performance in grooved channels with curved vanes. They showed that heat transfer is increased by a factor of 1.5–3.5 due to increased flow velocities in the grooved region when compared to the basic grooved channel. However, the results also showed that there is a significant increase in the pressure drop penalty.

Ridouane and Campo [11] performed a numerical study on laminar air flows in dimpled parallel-plate channels using finite volume method. They studied two configurations, one with symmetrically opposing cavities onto the bottom and upper walls and another with non-symmetric or staggered cavities onto the two parallel walls. They showed that the staggered arrangement makes insignificant differences in heat transfer enhancement and pressure drop when compared to symmetric configuration. Their results also showed that there exists an optimum value for the ratio of cavity depth to cavity print diameter in which the largest heat transfer rate from the wall is achieved.
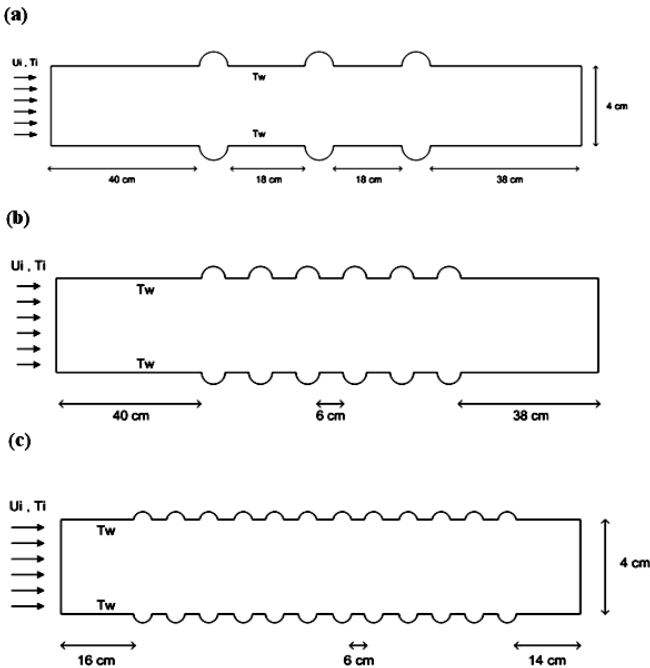

Fig. 1 Schematic of the channels interior section: (a) 3-cavity channel, (b) 6-cavity channel, and (c) 12-cavity channel

Won and Ligrani [12] and Park et al. [13] numerically investigated the turbulent air flow in channels with dimples placed on the bottom wall using the $k - \varepsilon$ turbulence model under the platform of the commercial code FLUENT. Bilen et al. [14] experimentally studied the heat transfer and friction characteristics of fully developed turbulent airflows in grooved tubes with three different geometric groove shapes. Their results showed that the maximum heat transfer enhancement in comparison with smooth tubes is obtained for the tubes with circular grooves, then the ones with trapezoidal and finally
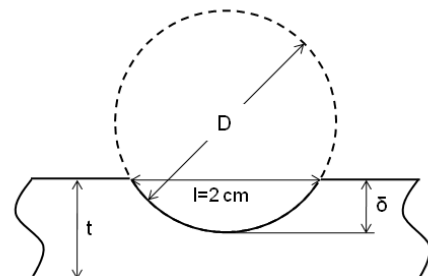
with rectangular grooves.

Although abundant studies have been accomplished in this field of research, but there are not many papers that have investigated the effect of channel wall conductivity on heat transfer characteristics. In this paper, conjugated heat transfer of air flow in parallel-plate dimpled channels is numerically simulated and the influence of Reynolds number, relative depth of cavities, the number of cavities, and the relative thermal conductivity of channel walls to the one of the fluid is investigated.

II. NOMENCLATURE

c_p	[J/kgK]	Fluid specific heat
D	[m]	Cavity curvature diameter
D_h	[m]	Hydraulic diameter
H	[m]	Channel Height
K	[W/mK]	Fluid thermal conductivity
k_w	[W/mK]	Thermal conductivity of channel wall
L	[m]	Dimple projection length
L	[m]	Length of each channel wall plus perimeter of cavities on it
N	[-]	Number of Cavities on each channel wall
Nu	[-]	Nusselt number
P	[Pa]	Fluid static pressure
q_w	[W/m²]	Wall heat flux
R	[m²/Ks²]	Gas constant
Re	[-]	Reynolds number
T_i	[K]	Fluid temperature at channel inlet
T_w	[K]	Wall temperature
t	[m]	Wall thickness
W	[m]	Channel width
$\vec{v}$	[m/s]	Velocity vector
δ	[m]	Cavity depth
μ	[kg/ms]	Fluid viscosity
ρ	[kg/m³]	Fluid density

III. CHANNEL GEOMETRY AND BOUNDARY CONDITIONS

Three channels containing series of 3, 6 and 12 transverse cavities symmetrically located on each wall are studied in this paper. All channels are 120 cm long and 4 cm high and their walls are 1 cm thick. The projection length (or print diameter) of the cavities is 2 cm. The distance between the cavities in three cases is not equal, considering the constant length of the channels. The schematic of channels under consideration and the geometric properties of cavities are illustrated in Fig. 1 and Fig. 2, respectively.

Fig. 2 Dimple geometry

Laminar incompressible air flow, with a density of 1.225

World Academy of Science, Engineering and Technology
International Journal of Mechanical and Mechatronics Engineering
Vol:5, No:1, 2011

kg/m3, viscosity of 1.7894×10-5 kg/ms and specific heat of 1006.43 J/kgK, enters the duct with a uniform velocity at constant temperature of T_i=280 K. No-slip condition is applied to the channel walls that are at constant temperature of Tw=320K. At the outlet the gauge pressure is set to zero as the boundary condition.

IV. GOVERNING EQUATIONS AND NUMERICAL METHOD

The governing equations are the continuity, momentum, and energy equations. The flow is studied under the following assumptions: steady-state, constant fluid properties and no natural convection and body forces. With these assumptions the governing equations as well as the ideal gas equation of state can be written as follows:

$$\nabla.(\rho\vec{v}) = 0 \tag{1}$$

$$\nabla.(\rho\vec{v}\vec{v}) = -\nabla p + \nabla.(\mu\nabla\vec{v}) \tag{2}$$

$$\nabla.(\rho c_p \vec{v} T) = \nabla.(\nabla.kT) \tag{3}$$

$$p = \rho RT \tag{4}$$

The commercially available computational package, FLUENT, is used for the numerical model. In this software, the partial differential equations governing the problem are reduced to a system of algebraic equations using finite volume procedure. The discretization of the convective and diffusive fluxes across the control surfaces is modeled using the QUICK scheme and the pressure-velocity coupling is handled with the SIMPLE method. Quad cells are used to discretize the problem domain with a structured mesh. Grid points are distributed in a non-uniform manner with a higher concentration near the walls due to higher variable gradients expected in these locations. The convergence criterion is that the residual variations of the mass, momentum and energy conservation equations become less than 10^{-8}.

To study the effect of grid fineness on the solution, the process of mesh refinement is repeated progressively until insignificant changes in the field variables happen.

The numerical model is validated by solving the velocity and temperature fields in a parallel plate channel with smooth surfaces, constant inlet velocity and equal wall temperatures. For a fully developed condition the asymptotic value of $Nu_\infty = 7.54$ were found which is in good agreement with the Nusselt number reported in [15].

V. RESULTS AND DISCUSSION

Flow patterns, heat transfer characteristics, and pressure drop magnitudes have been studied numerically for flows through parallel-plate channels containing symmetrical arrays of hemi-cylindrical cavities of variable depth on their opposite walls. The results are compared to those for a channel with smooth surfaces.

Fig. 3(a) shows the streamlines and temperature distribution inside a dimple on the 3-cavitiy channel in Re=1000. The cavity has a relative depth of 0.5. It is located on the upper wall and is the closest one to the inlet. As can be seen in Fig. 3(a), a counterclockwise vortex is generated in the dimple (a

clockwise vortex is formed in each dimple on the bottom wall). The significant vortex effect on the temperature contours, especially at the trailing edge of cavity, is noticeable. Fig. 3(b) shows velocity vectors and velocity magnitude contours for the same case. As can be seen in this figure the local velocity magnitudes in the cavities are much lower than average velocity in the channel.
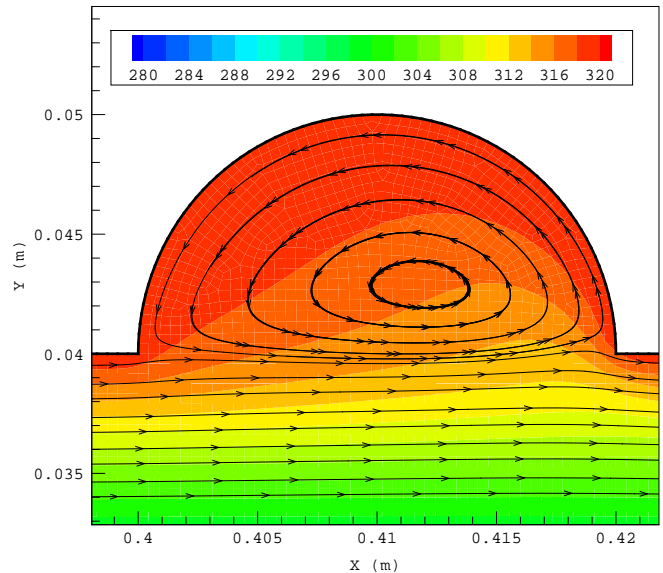

Fig. 3(a) Streamlines and temperature distribution (K) inside a dimple with δ/D=0.5 on the 3-cavity channel
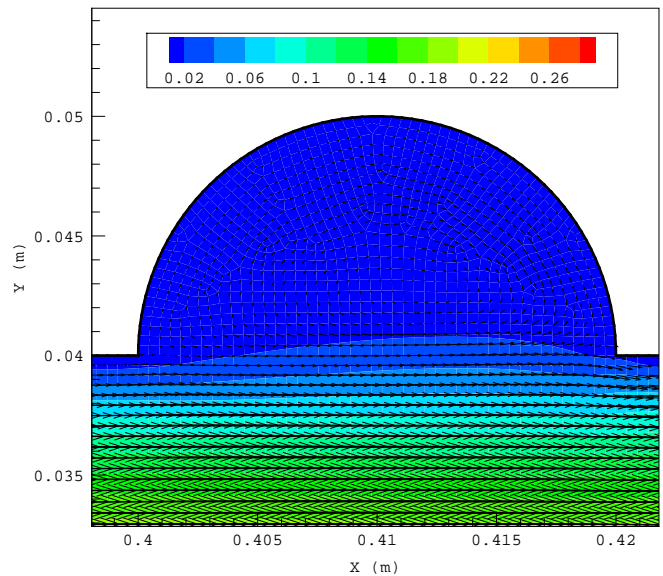

Fig. 3(b) Velocity vectors and velocity magnitude contours (m/s) inside a dimple with δ/D=0.5 on the 3-cavity channel

By increasing the Reynolds number to 2500 all velocities in the domain increase and as result the strength of vortexes increases. However, vortex structure remains the same in each dimple.

Temperature distribution, streamlines, velocity vectors and velocity magnitude contours inside a dimple with a relative

World Academy of Science, Engineering and Technology
International Journal of Mechanical and Mechatronics Engineering
Vol:5, No:1, 2011

depth of δ/D=0.2 on the 3-cavitiy channel in Re=1000, are illustrated in Fig. 4(a) and Fig. 4(b). The cavity is located on the upper wall of the channel and is the closest one to the inlet.
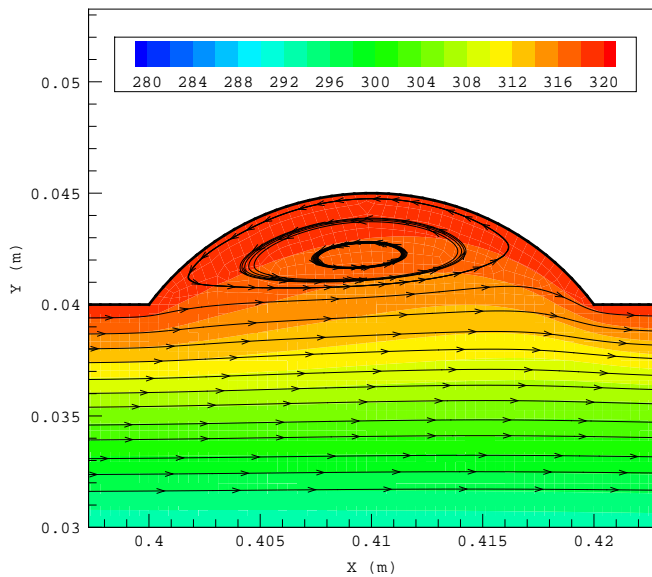

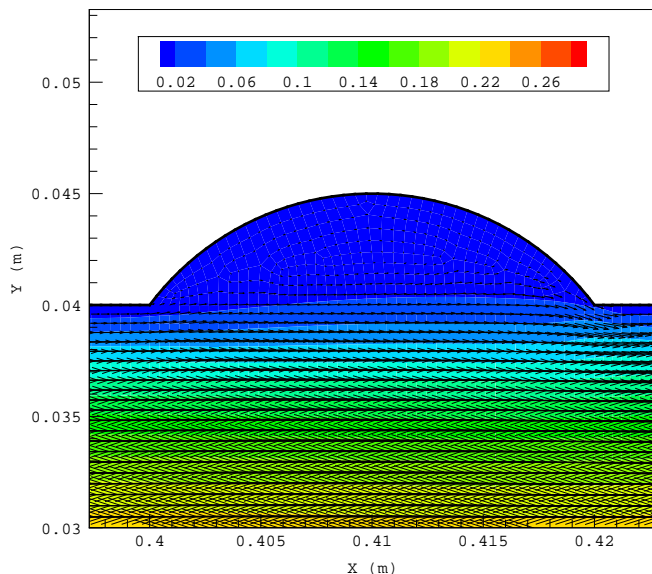Fig. 4(a) Streamlines and temperature distribution (K) inside a dimple with δ/D=0.2 on the 3-cavity channel

Fig. 4(b) Velocity vectors and velocity magnitude contours (m/s) inside a dimple with δ/D=0.2 on the 3-cavity channel

As can be seen in these figures, the vortex dimensions are smaller in this case than the case with relative depth of 0.5, but the velocity vectors are larger and as a result the vortex strength is of greater value. In other words, as the relative depth decreases from 0.5 to 0.2 the vortex strength increases.

Comparing Fig. 4(a) and Fig. 3(a), one can states that in the second case (δ/D=0.2), the wall heat flux is larger than the first case (δ/D=0.5) due the thinner thermal boundary layer and larger temperature variations near the wall.

To study the heat transfer characteristics of the flow in parallel plate channels, the average values of wall heat flux and Nusselt number should be computed in each configuration. The average wall heat flux is computed by the following equation:

$$\overline{q}_w = \frac{1}{L} \int_{wall} q_w(x) dx \qquad (5)$$

Where $q_w(x)$ is the wall heat flux and is defined based per unit area of the wall and L is the total length of the channel wall.

In a parallel-plate channel with smooth surfaces, wall heat flux has a maximum value at the inlet and decreases along the wall in an exponential manner as the hydrodynamic and thermal boundary layers develop. Variations of wall heat flux in dimpled channels, as presented in the following figures, have a more complex trend and for each dimple two peaks are observable. The maximum local heat flux happens at the downstream of each dimple which is due to large vorticities in these zones.
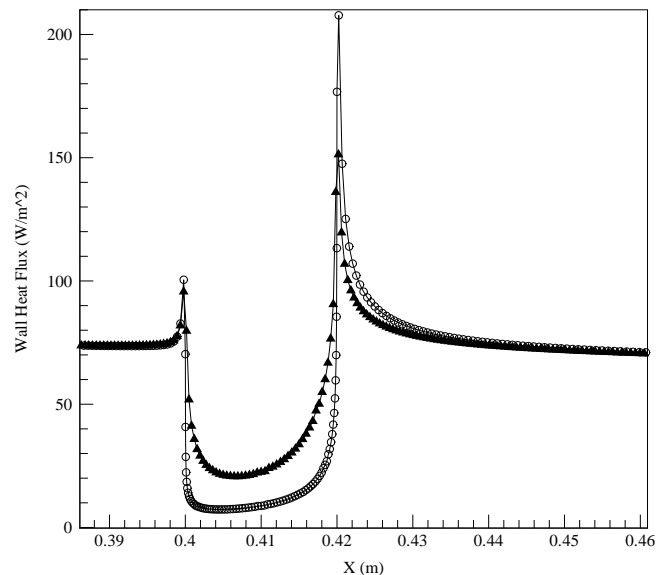

Fig. 5 Variations of heat flux along the bottom wall of the 3-cavity channel in Re=1000. Circle: δ/D=0.5, Delta: δ/D=0.2

Fig. 5 illustrates the variations of heat flux along the bottom wall of the 3-cavity channel for two different relative depths of dimples (δ/D=0.2 and 0.5). In this case, the Reynolds number equals 1000 and the variations are plotted only in the dimpled region closest to the inlet. Larger amounts of heat transfer enhancement in δ/D=0.2, which is noticed in Fig 5, are due to formation of stronger vortexes.

Similar results are obtained for the 12-cavity channel and are presented in Fig. 6. The bottom wall heat flux is plotted along the first three cavities closest to the inlet. As expected, dimples with relative depth of 0.2 outperform the ones with relative depth of 0.5. As can be observed in Fig. 6, the increase in heat transfer in the cavities closer to the inlet is more significant.
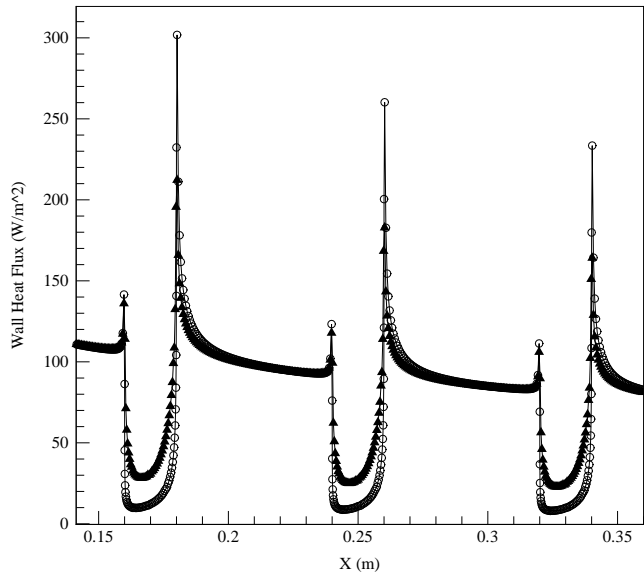
World Academy of Science, Engineering and Technology
International Journal of Mechanical and Mechatronics Engineering
Vol:5, No:1, 2011

Fig. 6 Variations of heat flux along the bottom wall of the 12-cavity channel in Re=1000. Circle: δ/D=0.5, Delta: δ/D=0.2

Fig. 7 shows the variations of the average Nusselt number as a function of Reynolds number in the 3-cavity channel with two different relative depths of dimples (δ/D=0.2 and 0.5).

The average Nusselt is computed by the equation:

$$\overline{Nu} = \frac{\overline{q}_w}{(T_w - T_i)}\left(\frac{D_h}{k}\right) \tag{6}$$

Where k is the Fluid thermal conductivity and D_h is the Hydraulic diameter and is computed by: $D_h = 4A/P = 2HW/(H + W)$, where H is the channel height and W is the depth of channel which is assumed to be unity in this study because of the two dimensional problem.
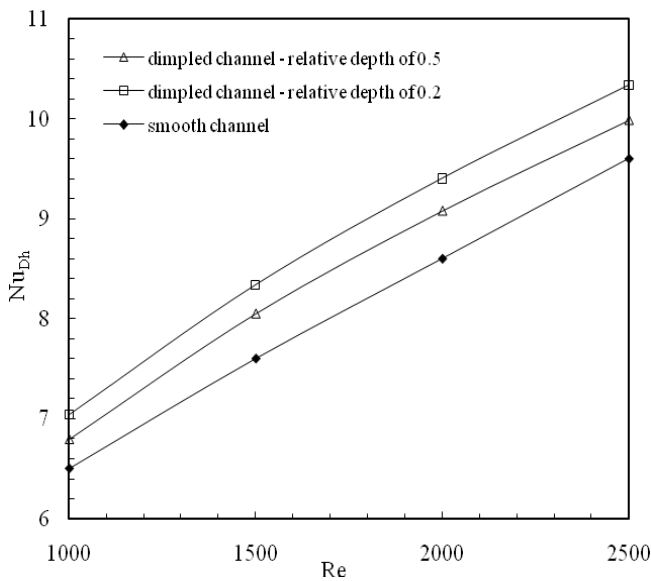

Fig. 7 Variations of Nusselt number as a function of Reynolds number in 3-cavitiy channel

Fig. 7 indicates that there is an increase in Nusselt number as the Reynold number increases. This trend is due to formation of stronger vortexes in cavities and also the reduction in thermal boundary layer thickness.

As it is presented in Fig. 8, the average Nusselt number is enhanced with an increase in the number of cavities in the cases with δ/D=0.2; however, a different trend is observed in the cases with δ/D=0.5. While δ/D=0.2 will be regarded as an optimum value for the relative depth in the following sections, it can be concluded that increasing the number of cavities has an amplifying effect on the average Nusselt number.
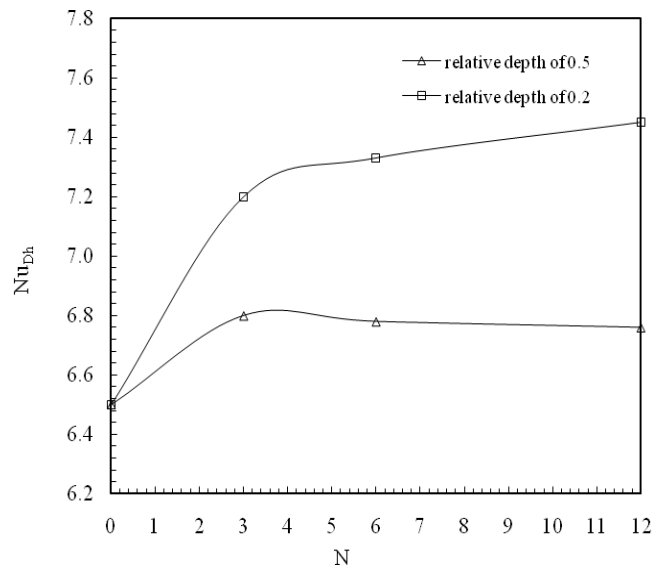

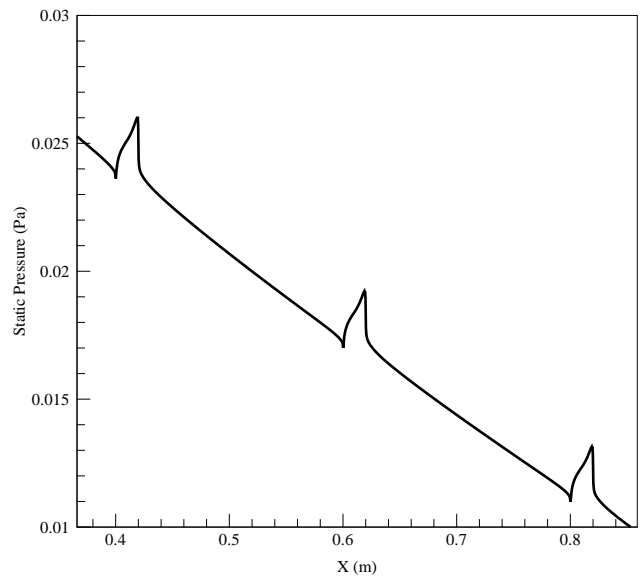Fig. 8 Variations of Nusselt number as a function of the number of cavities in Re=1000

Fig. 9 Variations of static pressure along the bottom wall of the 3-cavity channel with dimples of relative depth 0.2, in Re=1000

One of the consequences of an increase in the number of cavities is pressure drop. Static pressure in a smooth channel

World Academy of Science, Engineering and Technology
International Journal of Mechanical and Mechatronics Engineering
Vol:5, No:1, 2011

decreases with a constant slope along the main flow direction, though increasing the number of cavities results in abrupt static pressure drops in cavity locations. This effect is presented in Fig. 9, which shows the variations of static pressure along the bottom wall of the 3-cavity channel with dimples whose relative depths are 0.2, in Re=1000.

Another important factor in pressure drop increase is the Reynolds number augmentation. Fig. 10 shows the variations of pressure drop with Reynolds number in channels under consideration with dimples whose relative depth equals 0.2. As illustrated in Fig. 10, the pressure drop in the channel is amplified with an increase in the Reynolds number or the number of cavities.
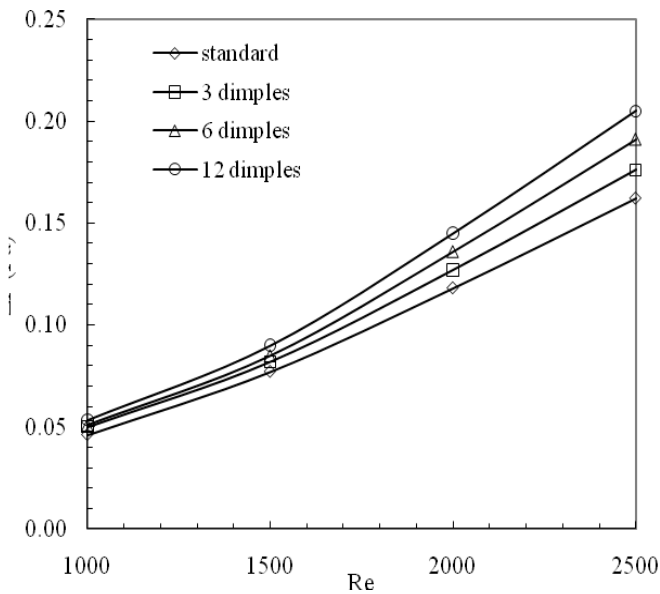
Fig. 10 Variations of pressure drop as a function of Reynolds number in channels with dimples of relative depth 0.2.

Considering the results presented in previous sections it can be concluded that as the relative depth of the cavities decreases, the heat transfer enhancement increases. However, as this value decreases to zero we have the same conditions as the smooth channel which has the lowest amount of heat transfer compared to dimpled channels; therefore, there must be an optimum value for the relative depth of dimples. To obtain this optimum value, Nusselt number is computed for different values of relative depth (0.1, 0.2, 0.3, 0.4, and 0.5) in the 3-cavity channel in two different Reynolds numbers. The results are illustrated in Fig. 11(a) and 11(b).

As it is clear in these figures, the optimum value of relative depth in which the maximum heat transfer is achieved, is about 0.2. In this value, the average Nusselt number is amplified between 10 to 12 percent compared to the case of parallel-plate channel with flat walls ($\delta/D=0.0$).

The last effect studied in this paper is the influence of heat transfer conjugation. In our simulations, the outer surfaces of channel walls are at constant temperature of 320 K and the inner ones are in coupled thermal interaction with the flowing air (heat is removed from these surfaces by forced convection due to the flowing air and it flows from outer surfaces to them by conduction in the solid wall). With these thermal boundary conditions, the study of conjugation effects is possible. The results of this study for the 3-cavity channel with dimples of relative depth $\delta/D=0.2$ are illustrated in Fig. 12. This figure shows the variations of wall heat flux with the ratio of thermal conductivity of channel walls to the one of the flowing fluid. To realize the metals which correspond to the values on the horizontal axis in Fig. 12, Table I is presented.
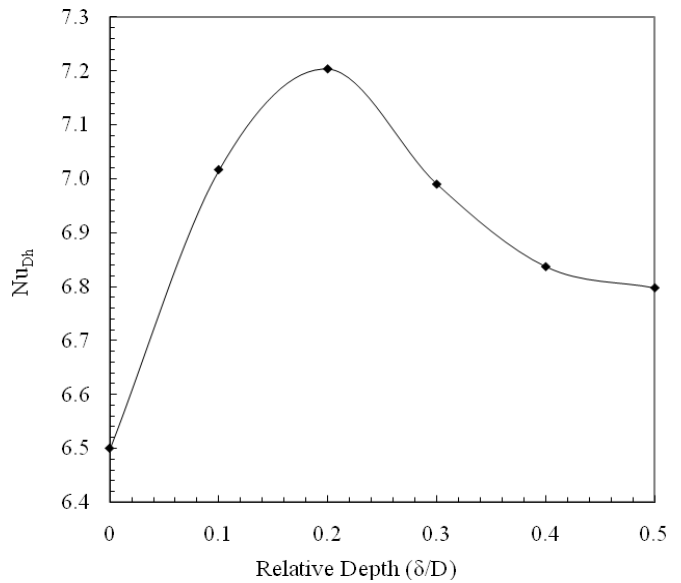

Fig. 11(a) Variations of average Nusselt number as a function of dimple relative depth in the 3-cavity channel in Re=1000
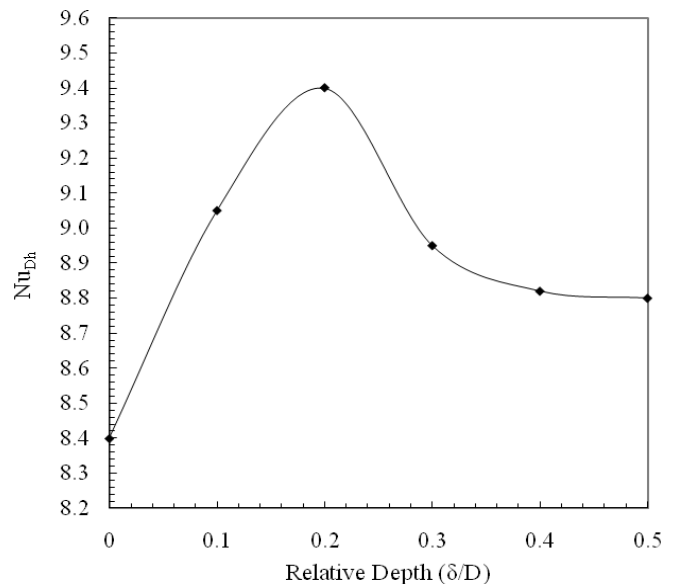

Fig. 11(b) Variations of average Nusselt number as a function of dimple relative depth in the 3-cavity channel in Re=2000

World Academy of Science, Engineering and Technology
International Journal of Mechanical and Mechatronics Engineering
Vol:5, No:1, 2011

As can be noticed in Fig. 12, when k_w/k is smaller than 250, an increase in this parameter results in a slight increase in the wall heat flux. However, the values of k_w/k smaller than 250, do not correspond to any common used metal in reality. Moreover, the figure shows that when this ratio is larger than 10^3 the steep of the plot becomes almost zero. Therefore, it can be stated that the overall influence of this ratio on wall heat flux is trivial and can be neglected. As a result, the other possible cases are not presented in this study.
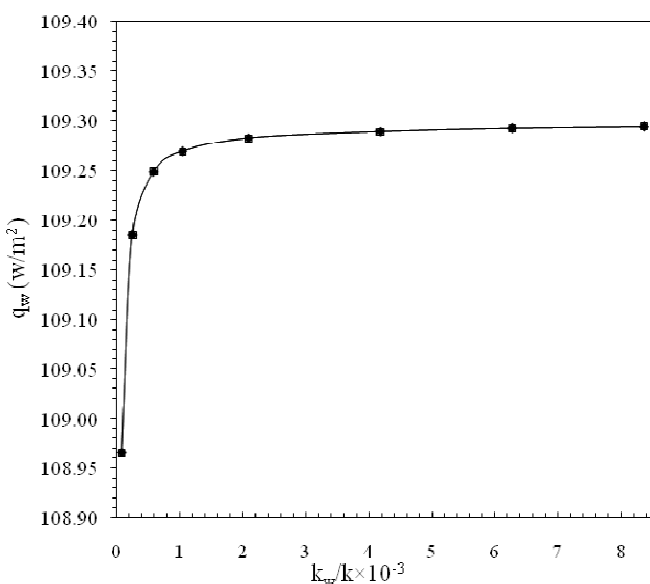

Fig. 12 Variations of the wall heat flux with the ratio of thermal conductivity of channel walls to the one of the fluid in the 3-cavity channel with dimples of relative depth $\delta/D=0.2$ in Re=2000

VI. CONCLUSION

Laminar airflows in parallel plate channels with cavities located on both walls are numerically studied. Velocity and temperature fields are computed to study the effects of the number of cavities and their relative depth on local structure of the flow and the heat flux distribution. Three different cases with 3, 6 and 12 hemi-cylindrical cavities located symmetrically on both channel walls are studied in Reynolds number ranging from 1000 to 2500.

The results showed an increase in strength of vortexes in cavities as the relative depth approaches to the value of 0.2. Because of the formation of these vortices, an enhancement in the local wall heat flux is observed especially in the downstream of each dimple. This effect causes the colder fluid move from central parts to the hotter zones of domain closer to the channel walls. This phenomenon is intensified as the relative depth approaches to its optimum value and increases the wall heat flux to its maximum value.

The results indicated that the mean Nusselt number increases as the Reynolds number increases. Moreover, the simulations showed an increase in the wall heat flux as the number of dimples is increased. In addition, the results depicted that the wall heat flux increases as the ratio of wall thermal conductivity to the one of the fluid increases, while this ratio remains smaller than 250. Though at larger values of this ratio, namely 10^3 and higher, the dependence of wall heat flux to the ratio becomes negligible. However, one can states that the overall effect of this ratio on wall heat flux is trivial and can be neglected.

TABLE I
VALUES OF THERMAL CONDUCTIVITIES FOR A NUMBER OF COMMON METALS

Metal	T (oC)	k W/(m K)	kw/k
Aluminum, pure	20	204.3	8440
	93.3	214.6	8870
	204.4	249.3	10300
Aluminum Bronze	20	76.2	3147
Carbon Steel, max 0.5% C	20	53.7	2217
Carbon Steel, max 1.5% C	20	36.4	1502
	400	32.9	1359
	1200	29.4	1216
Cartridge brass (UNS C26000)	20	120.1	4964
Cast Iron, gray	21.1	41.544 - 131.6	1716 - 5437
Chromium	20	90.0	3720
Cobalt	20	69.2	2861
Copper, pure	20	386.0	15951
	300	368.7	15236
	600	353.1	14592
Copper bronze (75% Cu, 25% Sn)	20	26.0	1073
Copper brass (70% Cu, 30% Zi)	20	110.8	4578
Iron, pure	20	72.7	3004
Silver, pure	20	406.8	16809
Stainless Steel	20	204.3	8440

REFERENCES

[1] Kelkar, and K. M., Patankar, S.V., 1987, "Numerical prediction of flow and heat transfer in a parallel plate channel with staggered fins", J. Heat Transfer, 109, pp. 25-30.

[2] Lazardis A., 1988, "Heat transfer correlation for flow in a parallel plate channel with staggered fins", J. Heat Transfer, 110, pp. 801-802.

[3] Cheng C.H., and Huang W.H., 1989, "Laminar forced convection flows in horizontal channels with transverse fins placed in the entrance region", Num. Heat Transfer, 16, pp. 77-100.

[4] Ghaddar, N.K., Karczak, K.Z., Mikic, B.B., and Patera, A.T., 1986, "Numerical investigation of incompressible flow in grooved channels, Part 1. Stability and self-sustained oscillations", J. Fluid Mech., 163, pp. 99-127

[5] Ghaddar, N.K., Megan, M., Mikic, B.B., and Patera, A.T., 1986, "Numerical investigation of incompressible flow in grooved channels, Part 2. Resonance and oscillatory heat-transfer enhancement", J. Fluid Mech., 168, pp. 541–567

[6] Fahanieh, B., Herman, C., and Sunden B., 1993, "Numerical and experimental analysis of laminar fluid flow and forced convection heat transfer in a grooved duct", Int. J. Heat Mass Transfer, 36, pp. 1609-1617

[7] Moon, H. K., O 'Connel, T., and Glezer, B., 2000, "Channel Height Effect on Heat Transfer and Friction in a Dimple Passage", J. Eng. Gas Turbines Power, 122, pp. 307–313.

[8] Chyu, M. K., Yu, Y., Ding, H., Downs, J. P., and Soechting, F. O., 1997, "Concavity Enhancement Heat Transfer in an Internal Cooling Passage", Proceedings IGTI, Turbo Expo, Orlando, FL, 2–5, Paper No. 97-GT-437.

[9] Ligrani, P. M., Mahmood, G. I., Harrison, J. L., Clayton, C. M., and Nelson, D. L. , 2001, "Flow Structure and Local Nusselt Number Variation in a Channel With Dimples and Protrusions on Opposite Walls", Int. J. Heat Mass Transfer, 44, pp. 4413-4425.

[10] Herman, C., and Kang, E., 2002, "Heat transfer enhancement in a grooved channel with curved vanes", Int. J. Heat Mass Transfer, 45, pp. 3741-3757

[11] Ridouane, H., and Campo, A., 2007, "Heat transfer and pressure drop characteristics of laminar air flows moving in a parallel-plate channel with transverse hemi-cylindrical cavities", Int. J. Heat Mass Transfer, 50, pp. 3913-3924

[12] Won, S.Y., and Ligrani, P.M., 2004, "Numerical predictions of flow structure and local Nusselt number ratios along and above dimpled surfaces with different dimple depths in a channel", Num. Heat Transfer, 46, pp. 549-570

[13] Park, J., Desam, P.R., and Ligrani, P.M., 2004, "Numerical predictions of flow structure above a dimpled surface in a channel", Num. Heat Transfer, 45, pp. 1-20

[14] Bilen, K., Cetin, M., Gul, H., and Balta, T., 2009, "The investigation of groove geometry effect on heat transfer for internally grooved tubes", Applied Thermal Engineering, 29, pp. 753-761

[15] Incropera, F.P., and De Witt, D.P., 1996, "Fundamentals of Heat and Mass Transfer", fourth ed., Wiley